

Polymer Bonded Soft Magnetics for EMI Filter Applications in Power Electronics

S. Egelkraut, L. Frey
Chair of Electron Devices
University of Erlangen-Nuremberg
Erlangen, Germany

Email: sven.egelkraut@leb.eei.uni-erlangen.de
<http://www.leb.eei.uni-erlangen.de>

M. Rauch, A. Schletz, M. März
Fraunhofer Institute for Integrated
Systems and Device Technology (IISB)
Erlangen, Germany
<http://www.iisb.fraunhofer.de/>

Abstract—In this study, polymer bonded soft magnetic materials (PBSMM) were investigated for the application as a magnetic core and electromagnetic shielding material in inductive devices for EMI filter applications. The nature of switch mode power converters makes them a potential source of EMI noise emission. EMI filters are generally necessary to ensure electromagnetic compatibility of converters to the other electronic equipment. Conventional discrete EMI filters usually comprise passive components with different volume and form factors. The manufacturing of conventional inductive components requires different processing and packaging technologies, of which many include cost intensive processing steps. Due to the parasitics of the discrete components and their interconnections the effective filter frequency range is limited. As a result discrete EMI filters are usually not integrable into an arbitrary formed volume and show relative high production costs. This study aims on solving this issue by the integration of inductive EMI filter components using polymer bonded soft magnetics. PBSMMs were produced using thermoplastic polyamide 6 matrix materials. The filler materials were chosen from the wide range of different soft magnetics. The magnetic properties were characterized using injection molded ring core test specimens and a computer controlled hysteresis recorder as well as an impedance analyzer. Inductive devices with PBSMM as magnetic core have great potentials in automotive applications that have to meet a high geometric flexibility and highest power densities.

I. INTRODUCTION

Power electronics has been continuously improved by new semiconductor devices and materials, an continuously increasing switching frequency and advanced integration technologies. The need for high integration level, high performance, and reduced production costs of power electronics is the driving force for polymer bonded soft magnetics inductor technologies. Especially in automotive applications the space requirements and the possibility to form the devices without any restrictions in the outer form is one outstanding argument for the use of polymer bonded inductive components. Recent studies on polymer bonded soft magnetic materials showed the perspective to produce soft magnetics with a high saturation flux density, useful permeability values, and low coercivity for low frequency applications [1]. Metallic materials like Fe-Si3 [2], [3] or nano crystalline FeSiBCuNb [4], [5] show good magnetic properties with the capability of processing these materials with conventional polymer processing technologies. Polymer bonded soft magnetics were investigated for planar

transformer production [6] and verify the possibility to build up flat and integrated power converter for example for gate driver applications.

Any switching electronic device is a potential EM noise source. High level electromagnetic disturbances may cause electronic systems to malfunction in a common electromagnetic environment [7].

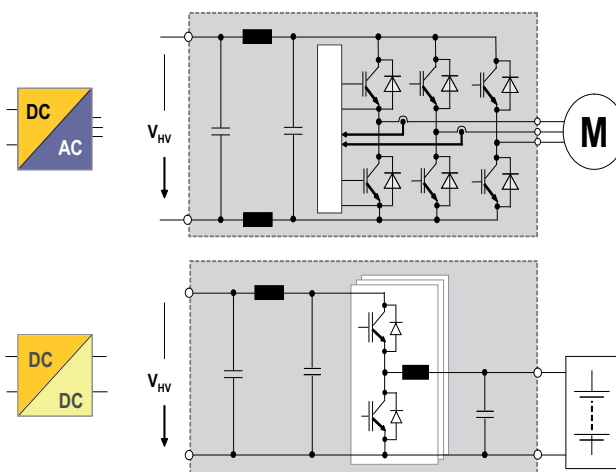


Fig. 1. EMI filter applications in power electronics

Conventionally, EMI filters are normally implemented by using discrete conventional components. The total volume of such an assembly is dominated by the passive components and the dead volume between the chunky devices. Schematics of two typical EMI filter structures are shown in Fig. 1. Film capacitors enable the integration of capacitive devices into a volume but with strictly restrictions on the outer form of this. So the effective degrees of freedom in the form of these devices are limited by the processing technology but they are much larger than for example of electrolytic capacitors. The integrated hybrid drive presented in [8] e.g. uses a ring-shaped dc link capacitor in order to achieve an optimum filling of the available package volume. This capacitor has been developed in cooperation with the Epcos AG and provides a capacitance of 500 μ F (450V).

Recent studies on integrated inductive devices focus on

power converters and therefore mostly on planar structures and low power applications. [9], [10]. The aim of this study was to produce and characterize polymer bonded soft magnetics with application adapted magnetic properties and to realize inductive devices for high frequency EMI filter applications using these materials. The following demands and targets have been specified for the exemplary EMI filter made of polymer bonded soft magnetics:

- An optimal use of the available space
- The potential to produce the device at lower production costs with highly efficient production processes
- An ampacity for high DC currents up to 125 A
- An attenuation sufficient to push the noise below the limits for conducted emissions as defined in several standards

II. EMI CHARACTERIZATION AND FILTER TOPOLOGY

The integrated hybrid drive described in [8] was characterized regarding its EMC behavior in order to estimate the necessary attenuation characteristic of the EMI filter. Only conducted differential mode emissions were considered, because any other emissions are highly depending on the overall system configuration. The drive unit was mounted on an emotor test bench for the characterization under various torque and speed load conditions. To avoid any interference with heavyduty electronic power supplies, the drive was fed from a NiCd battery pack, configured for a nominal voltage of 288 V, and capable to provide energy of up to 8 kWh. The DC link voltage noise was measured close to the DC link capacitor using both a spectrum analyzer (R & S FSP3 with FSP-B29) and an oscilloscope (Tektronix TDS5034B). An AC coupling capacitor and an attenuator (20dB) were inserted to protect the spectrum analyzer, the additional attenuation is considered in Fig. 2. The DC link current was measured using a Tektronix current probe TCP303 with TCPA300. Fig. 2 shows the DC link voltage ripple under maximum load, with a speed of 1500 rpm corresponding to a fundamental frequency (f_0) of the inverter output current of 200 Hz; the switching frequency (f_s) of the inverter is 8 kHz.

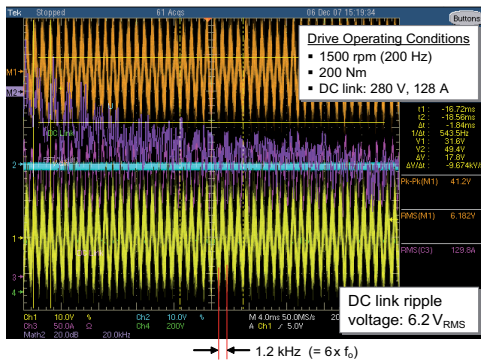


Fig. 2. DC link ripple voltage

Fig. 3 shows the spectrum up to 10 MHz. According to the limiting lines given in Fig. 3, an attenuation of about 22 dB

at 2.2 MHz is necessary to push the noise below the limits defined, e.g., in the Daimler standard DC 10614.

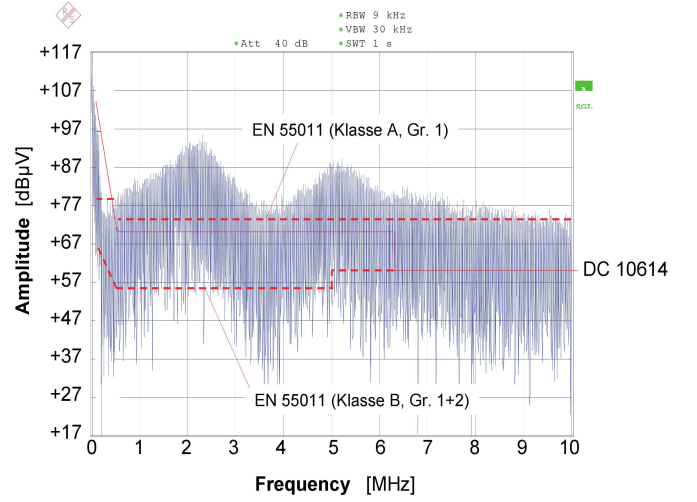


Fig. 3. Spectrum of the conducted DC link voltage noise with some limiting lines

Fig. 4 depicts the AC equivalent circuit of the drive inverter including the chosen filter topology, the high-voltage cable L_{La} and L_{Lb} , and the electrical parameters of the battery system v_{bat} and R_i . L_{1a} and L_{1b} are the filter inductors presented in this paper.

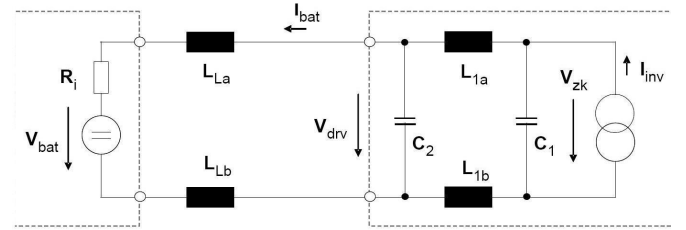


Fig. 4. Inverter with chosen EMI filter topology and HV supply equivalent circuit. C_1 is the main DC link capacitor. The available space allows a maximum capacitance of $60\mu F$ for the filter capacitor C_2

III. MATERIALS AND PROCESSES

This chapter presents the used materials, processes and the measurement equipment.

A. Filler Materials

Magnetic materials can be divided into different groups depending on their magnetic properties. Iron, cobalt, and nickel based metallic alloys like FeSi, NiFe, and CoFe show a high saturation flux density (2.35 T for CoFe) and a high permeability at low frequencies. These properties are well suited for e.g. EMI filters and low frequency chokes. The most effective manner to produce metallic powders is the water or gas atomization. The final particles have a spherical geometry shown in Fig. 5 resulting in a low viscosity of the polymer - filler compound. For our PBSMM investigations, an iron powder (FeSi6.8 from Höganäs) was used. The saturation

inductance of bulk material test specimens made of this material is 1.6 T.

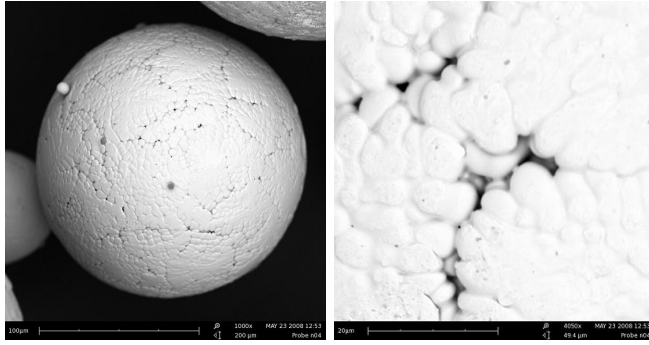


Fig. 5. SEM pictures of the water atomized FeSi6.8 powder right: surface structure

B. Polymers and Processing

The polymer matrix materials was an Ultramid B27 from BASF, an semicrystalline thermoplastic material. It has a low viscosity and good thermal and mechanical properties regarding the present application. A PA6 containing 20vol.%, 40vol.%, 50vol.%, 60vol.% and 65vol.% filler powder was prepared in a twin screw extruder. Polymer injection molding is a production process for manufacturing components from thermoplastic and thermosetting plastic materials and was used for the plastic molding. An injection molding tool was used for ring core test specimens' production. A picture of the molding tool is shown in Fig. 6 left.

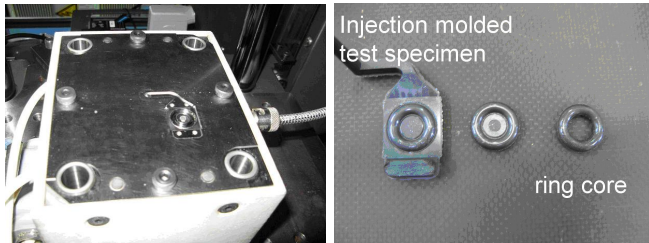


Fig. 6. Injection molding tool and test specimens

Polymer pressure molding was used for the inductive device manufacturing in order to reduce the costs for a complex injection molding tool. This process consists of filling the tool with the polymer compound and pressing the final device in a vacuum oven.

C. Magnetic Characterization

Toroidal cores were chosen due to the homogenous field distribution resulting in an accurate measurement. The magnetic permeability was measured with a precision impedance analyzer for frequencies up to 100 MHz (Agilent 4294A). The magnetic losses were measured with a computer controlled hysteresis recorder similar to that described in [11]. A schematic of this recorder is shown in Fig. 7.

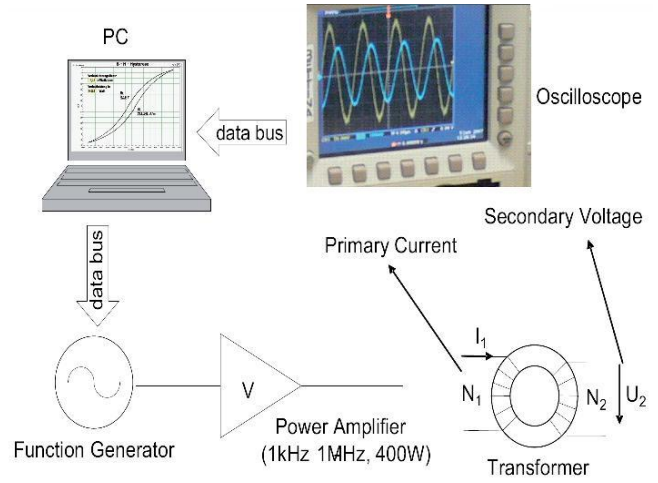


Fig. 7. Hysteresis recorder

The specific magnetic hysteresis power losses per volume are related to the area of the hysteresis curve and the frequency, and can be expressed by the following equation:

$$\frac{P}{V} = f \cdot \oint H \partial B \quad (1)$$

where f is the frequency of the applied field, H the magnetic field strength, and B the magnetic flux density. The saturation flux density was measured using a vibrating sample magnetometer (VSM).

IV. MATERIAL CHARACTERIZATION RESULTS

The measurements of the magnetic properties were performed using toroidal test specimens with an effective magnetic length of 40 mm and a core cross-section area of 11.3 mm² with a winding comprising 10 turns. The test specimens are shown in Fig. 6 right.

A. Frequency Characterization

The permeability of the polymer bonded soft magnetics was calculated from the measured inductance of the ring cores. The investigations showed only a small deviation in the value of the inductance over a number of 30 test specimens. Therefore constant filler contents in all test specimens can be assumed. The permeability of the polymer bonded soft magnetics depends on the filler content and increases with increasing filler fraction up to 30 at a measurement frequency of 10 kHz. The polymer compounds with the spherical FeSi6.8 filler particles show a low viscosity of the polymer melt. This results in high processable filler fractions up to 65 vol.%. The resulting permeability stays quite constant up to a frequency of around 1 MHz for highest filler fractions. The permeability measurements of the test specimens are given in Fig. 8.

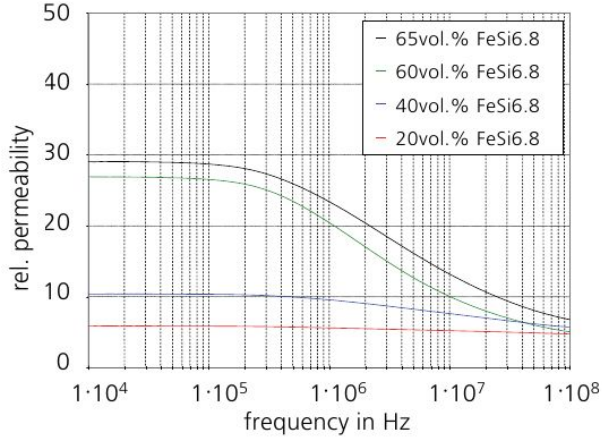


Fig. 8. Rel. permeabilities of the polymer compounds

B. Saturation Flux Density

The measurement was done using a vibrating sample magnetometer (VSM). For this purpose the test specimens were physically vibrated sinusoidally in an outer magnetic field. The induced voltage in the pickup coil was measured and is proportional to the sample's magnetic moment.

The volume of the ring cores was assumed to be totally magnetic even if the compound shows a defined filler fraction of the magnetic material. This was done in order to measure the saturation inductance of the total compound volume and not of the filler material itself. The measured values are given in Tab. I. In comparison to other magnetic materials for high

TABLE I
 B_{Sat} OF THE POLYMER COMPOUND AT A GIVEN FILLER FRACTION

Filler fraction	20	40	50	60	65
B_{Sat} FeSi measured	0.29	0.59	0.72	0.89	0.97

frequency applications this saturation values are between the ferrites with nearly 500 mT and the pressed iron powder cores with up to 1.6 T.

C. Power Losses

In the case of magnetic materials, losses are attributed to three physical mechanisms [14]. The different energy losses per cycle are given by:

$$W = W_h + W_{cl} + W_{exc} \quad (2)$$

W_h represents the hysteresis losses for quasi static frequencies which are assumed to be constant with frequency. W_{cl} represents the eddy current losses which are directly connected with the electrical conductivity of the magnetic material. W_{exc} represents the losses due to the high frequency dynamic movements of the magnetic domains. The measured losses of the FeSi filled PBSMMs are shown in Fig. 9, all losses

are referred to the total core volume. The magnetic area was defined as the geometric crosssectional area of the toroidal core. At a given macroscopic flux density, PBSMMs generally reveal higher power losses per volume than the corresponding soft magnetic raw materials. Since the magnetic particles are dispersed in a polymer matrix, the effective magnetic cross section is lower depending on the filler content. In addition,

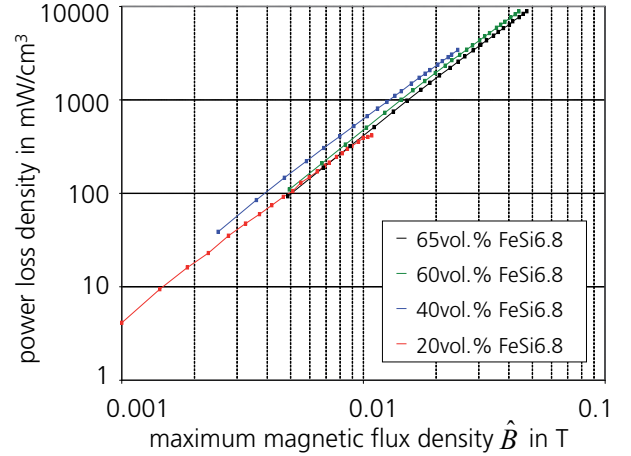


Fig. 9. Power losses of FeSi6.8 filled PBSMMs

compared to solid soft magnetics there is no homogeneous flux density across the total cross section of a PBSMM toroidal core. This leads to an increased magnetic flux density in the magnetic particles, and thus to increased power losses. This fact gains influence especially for particles which are in touch with each other. The magnetic flux takes lines of least magnetic resistance and hence the flux density exaggerates in the points of contact between the particles. This flux density concentration is expected to be a dominating power loss source for the spherical filler particles at a filler fraction around 40 vol.% and results in an increasing of all loss mechanisms. Especially eddy current losses increase with increasing electrical conductivity. At lower filler fractions the particles are not in touch with each other and each particle is covered by an insulating polymer layer. With increasing filler content more and more particles get in contact.

At filler fractions around 40 vol.% magnetic and electric paths through the magnetic material arise from the particles touching each other. These magnetic and electric percolation networks show only a small effective magnetic and electric area. At higher filler contents the effective magnetic area increases and therefore the power losses due to the magnetic flux density concentration decrease. Pictures of the particle distribution at different filler fractions are given Fig 10.

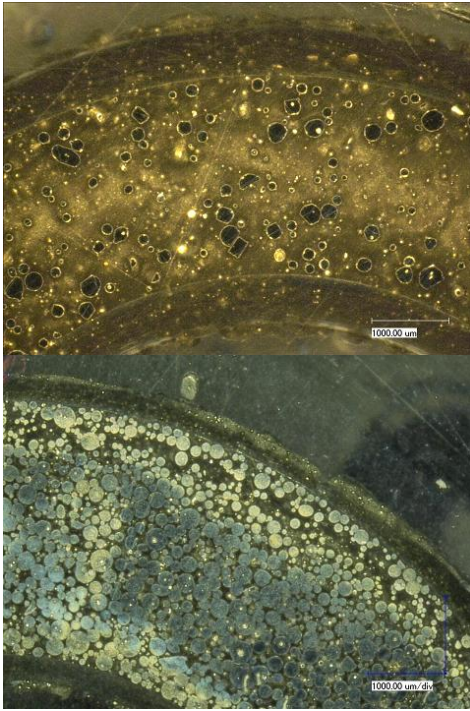


Fig. 10. Cross sections of the FeSi filled polymer ring cores at 20 vol.% (top) and 60 vol.% (bottom)

V. ELECTROMAGNETIC DESIGN OF THE EMI FILTER DEVICE

Inductive devices made of PBSMM don't feature predefined and catalogued geometries. For different winding arrangements in the given construction space the effective magnetic parameters like the effective magnetic area or the magnetic length, the inductance and the maximum flux density were calculated using an electromagnetic FI (finite integration) simulation software (CST-EM-Studio).

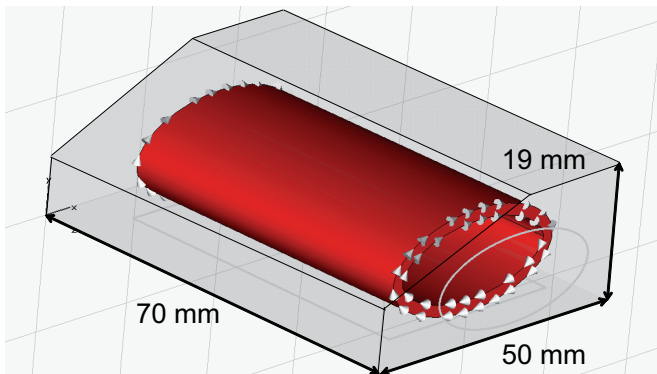


Fig. 11. Simulation geometry A

The complexity of the manufacturable design was simplified

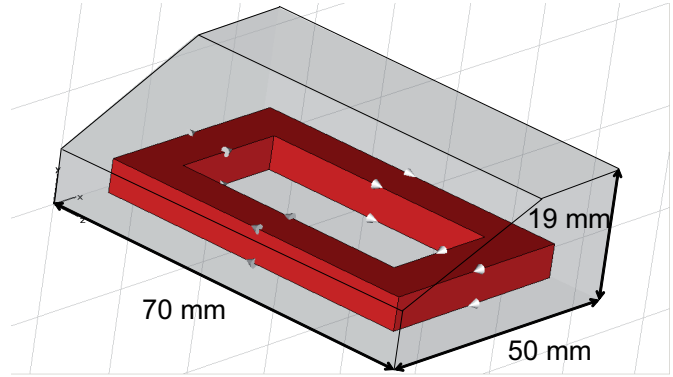


Fig. 12. Simulation geometry B

in order to reduce the simulation time. The windings of the inductor were simulated using a predefined function reducing the physical windings to a current carrying volume with a chosen number of turns. The goals of these simulations were:

- Calculation of the inductance and the maximum flux density of the magnetic material in the predefined volume.
- Choosing that winding geometry with an optimal B-field distribution

Winding geometries analyzed in the following are:

- Spiral winding normal to the base plate with a magnetic flux orientation in the longitudinal axle of the inductor as shown in Fig. 11.
- Rectangular winding parallel to the base plate with a magnetic flux orientation normal to the base plate as shown in Fig. 12.

The simulation results show that the simulation geometry A realizes a more homogenous field distribution. The effective magnetic area is nearly constant over the total magnetic length. Therefore the magnetic flux density shows no local concentration. The simulation geometry B shows higher maximum flux densities due to local flux concentration resulting in higher power losses. In addition these simulations disqualify the Vitroperm fillers for the given application due to the reduced saturation inductance in comparison to the FeSi filled polymer. The simulation results are shown in Fig. 13.

In addition to the flux density the inductance was calculated for the two winding geometries in order to estimate the required filler fraction for the soft magnetic polymer. The simulation results are shown in Fig. 14.

The simulation illustrates that permeability values higher than 22 are sufficient to produce an inductor with an inductance higher than our target value of $5 \mu\text{H}$. The usage of a material with a permeability of 28 like it was measured for the 60 vol.% FeSi filled polymer results in an inductance of $6.5 \mu\text{H}$ for the simulation geometry A. The simulation results for this material predict a maximum flux density lower than 0.6 T which is much lower than the measured saturation

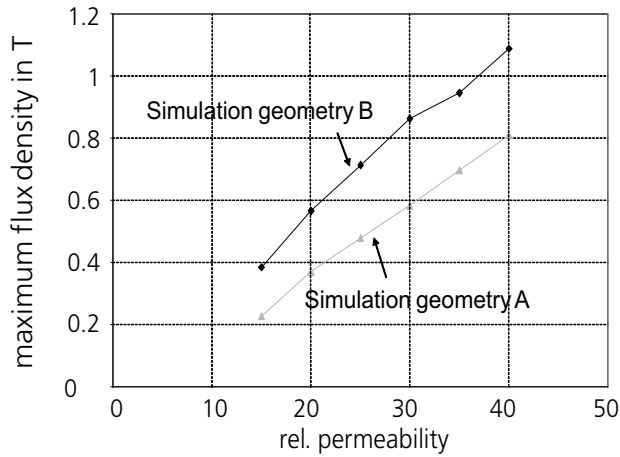


Fig. 13. Max. flux density B_{max} in T vs. permeability

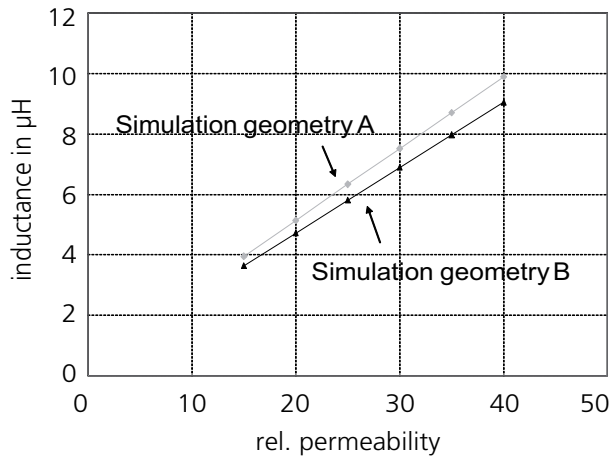


Fig. 14. Simulated inductance L vs. permeability

inductance of 0.89 T. Therefore the simulation results verify the possibility to produce powerful inductive devices for EMI filters using polymer bonded soft magnetics.

VI. MECHANICAL DESIGN

An elliptic crosssection of the coil was chosen in the electromagnetic simulations as it utilizes the available volume best. The radii of the coil shown in Fig. 11 are $a=16.5$ mm and $b=7.5$ mm (measured from the core centre to the centre of the wire). The wire has a cross section of 6×2 mm² as it is required for carrying a mean current of 125 A. To satisfy the process and reliability requirements a wall thickness of 2 mm from the coil surface to the outer device wall was chosen. The area of the final manufactured ellipse was reduced insignificantly in order to ensure this wall thickness. To ensure high voltage insulation the copper wire was insulated by a polymer finish. A plastic cap was constructed in order to realize the electric contact between the device and the electronic environment using two screws. The total mechanical design is given in Fig. 18. For the realization of a prototype choke, a polymer pressure molding

tool was constructed based on the mechanical design of the inductive device.

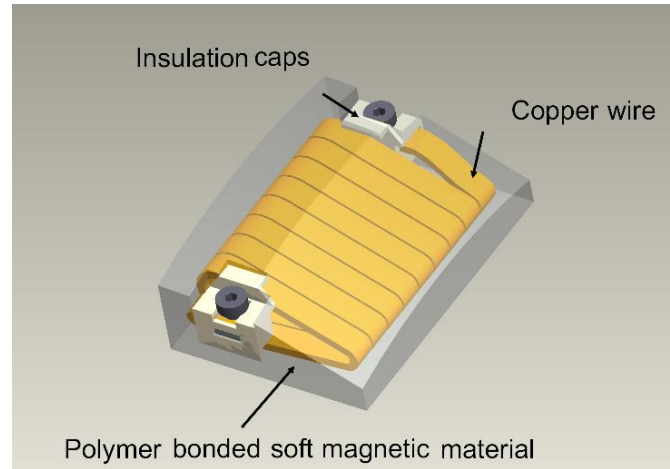


Fig. 15. Mechanical design

VII. THERMAL DESIGN

The aim of the thermal simulation was the calculation of the maximum allowable power losses to ensure a maximum operating temperature of 125°C for the polymer matrix. The thermal conductivity of the polymer compound strongly depends on the filler, the polymer matrix and the temperature. Values from 0.5 W/mK up to 10 W/mK are known for highly filled polymers in the literature [15]. Due to the high filler fraction and the spherical filler geometry a linear increasing of the thermal conductivity from 1 W/mK up to 4 W/mK with an increasing filler fraction 20 vol.% up to 65vol.% was expected [16] and taken as a input parameter for the simulations. For the simulation the temperature of the water cooled heat sink was set to 90°C in order to simulate the later application. The ohmic losses at an rms current of 125 A were calculated to 20 W. The contact layer between the inductive device and the cooling channel was modeled with a thermal conductance value of $k=10$ W/mm² K (assuming a layer of conductive adhesive with a thickness of $d=0.05$ mm and a thermal conductivity of $\lambda=5$ W/m K). The contact layer between the encapsulation and the coil has a thermal conductance value of $k=0.4$ W/mm² K (assuming a layer of isolation resin with a thickness of $d=0.5$ mm and a thermal conductivity of $\lambda=0.2$ W/m K). For the simulation the magnetic power losses were varied from 0 W up to 80 W depending on the load state of the synchronous drive.

The simulation results shown in Fig. 16 illustrate that a thermal conductivity of 3 W/mK is sufficient to dissipate a total power loss of 80 W and a magnetic power loss of 60 W. The possibility to produce inductive devices closely thermally coupled to heat sink structures as a result of the great degree in geometric freedom is a great advantage of polymer bonded soft magnetics.

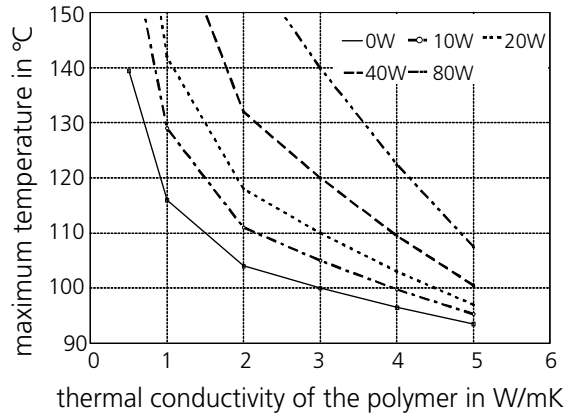


Fig. 16. Thermal simulation results

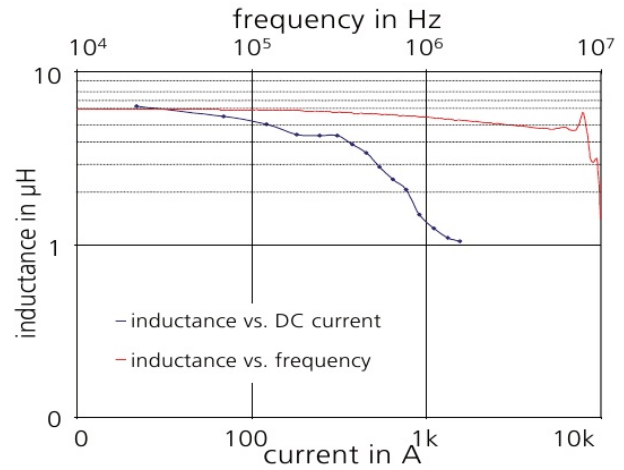


Fig. 18. Electrical characterization results

VIII. MEASUREMENT RESULTS

A photograph of the produced device is given in Fig. 17.

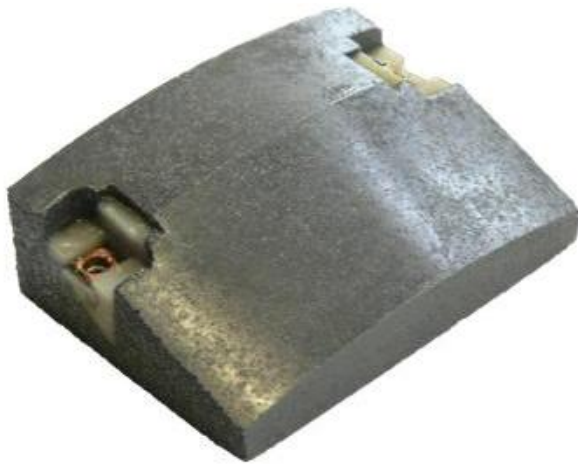


Fig. 17. Photograph of the inductive filter device made of PBSMM

The inductance characterization results like they are shown in Fig. 18 clearly demonstrate the high frequency applicability for the recommended inductive device. The inductance reaches a maximum value of $6.1 \mu\text{H}$. According to the simulation this corresponds to a permeability of 26 and therefore a filler content of 58vol.% of the iron silicon filler material. The inductance decrease slightly to $4.2 \mu\text{H}$ at 7.2 MHz and shows a resonant frequency around 8MHz.

The presented inductive device shows a soft saturation of the magnetic material, due to the fact that each soft magnetic iron particle shows an individual flux density distribution depending on its geometric parameters, its location in the device volume and its distance to other particles. At a DC current of 125 A, as it is required by the application, an inductance of $5 \mu\text{H}$ is attached. The saturation of the total soft magnetic volume requires a current higher than 1000 A.

The saturation behaviour of the presented device is shown in Fig. 18.

IX. CONCLUSION

This paper presents the characterization of polymer bonded soft magnetics and a design flow for an inductive device for EMI filter applications made of these materials. The EMI filter is used to attenuate the conducted electromagnetic noise on the DC link of an inverter of a hybrid drive. The concept of inductive devices using polymer bonded soft magnetics could be presented. These materials were investigated in order to manufacture filter inductors using production processes of polymer technology and therefore to realize complex formed devices nearly without restrictions in the outer form for automotive applications. It could be shown that polymer compounds filled with high filler fractions of soft magnetic particles fulfill soft magnetic requirements for power electronics filter applications regarding the parameters permeability, power losses and saturation flux density. A mechanical, electromagnetic and thermal design flow was done for a concrete demonstrator with a very complex construction space. All these simulations show the possibility to manufacture inductive devices using soft magnetic polymer compounds. The advantages of polymer bonded soft magnetics for the presented application are:

- The air gap is distributed in the total core volume. This results in a reduced stray field and a very soft saturation.
- The polymer EMI filter fits into the predefined space and fills in the blank between the water cooled heat sink and the outer clutch box. So no additional mechanical fixation or filling polymer is needed for a reliable assembly.
- The EMI filter is directly attached on the water cooled heat sink and shows planar surfaces. Therefore an optimal distribution of thermal energy is ensured.
- The power losses of the soft magnetic polymer are higher than for ferrite or metallic bulk materials producing a higher attenuation at high frequencies for the EMI filter.

ACKNOWLEDGMENT

The author would like to thank the Deutsche Forschungs Gemeinschaft (DFG) and the Sonderforschungsbereich 694 (SFB) as well as the European Center for Power Electronics (ECPE) for the financial support of this work.

REFERENCES

- [1] M. Anhalt, B. Weidenfeller, "Dynamic losses in FeSi filled polymer bonded soft magnetic composites", *J. Magn. Magn. Mater.*, vol.304, pp. 549-551, 2006
- [2] M. Wulfa, L. Anestiev, L. Dup, L. Froyen, J. Melkebeek, "Magnetic properties and loss separation in iron powder soft magnetic composite materials", *Journal of Applied Physics*, vol. 91, no. 7845, (2002)
- [3] B. Weidenfeller, M. Anhalt, W. Riehemann, "Variation of magnetic properties of composites filled with soft magnetic FeCoV particles by particle alignment in a magnetic field", *J. Magn. Magn. Mater.*, vol. 320, pp. 362-365, (2008)
- [4] R. Lebourgeois, S. Brenguer, C. Ramiarinjaona, T. Waeckerl, "Analysis of the initial complex permeability versus frequency of soft nanocrystalline ribbons and derived composites", *J. Magn. Magn. Mater.*, vol. 254-255, pp. 191-194, (2003)
- [5] F. Alves, C. Ramiarinjaona, S. Brenguer, R. Lebourgeois, and T. Waeckerl, "High-frequency behavior of magnetic composites based on FeSiBCuNb particles for power electronics", *IEEE Trans.Magn.* vol.38, issue. 5, pp. 3135 - 3137, (2002)
- [6] S. Egelkraut, M.März, H. Ryssel, "Polymer bonded soft magnetic particles for planar inductive devices", *Proc. of the 5th International Conference on Integrated Power Systems (CIPS)*, Nuremberg, Germany, pp. 167-174, (2008)
- [7] R. Chen, J.D. van Wyk, S. Wang, W.G. Odendaal, "Application of Structural Winding Capacitance Cancellation for Integrated EMI Filters by Embedding Conductive Layers", *IEEE Industry Applications Conference*, vol. 4, pp. 2679- 2686, (2004)
- [8] M. März, M. H. Poech, E. Schimanek, A. Schletz, "Mechatronic Integration into the Hybrid Powertrain - The Thermal Challenge", *Proc. 1th International Conference on Automotive Power Electronics (APE) 2006*
- [9] E.J. Brandon, E.E. Wesseling, V. Chang, W.B. Kuhn, "Printed microinductors on flexible substrates for power applications", *Trans. Compon. Packag. Technol.*, IEEE, Volume 26, Issue 3, Sept. 2003
- [10] E. Waffenschmidt, "Printed circuit board integrated multi output transformer", *Proc. 5th International Conference on Integrated Power Systems*, Nuremberg, 2008.
- [11] DIN EN 60404-6 European Standard
- [12] M. März, E. Schimanek, M. Billmann, "Towards an Integrated Drive for Hybrid Traction", *CEPS Workshop: From Success to Significance* (2005)
- [13] A.W. Kelly, F.P. Symonds, "Plastic-iron-powder distributed air gap magnetic material", *IEEE Power Electronics Specialists Conference (PESC)*, (1990)
- [14] A. Boglietti, A. Cavagnino, M. Lazzari, and M. Pastorelli, "Predicting iron losses in soft magnetic materials with arbitrary voltage supply - An Engineering Approach", *IEEE Trans. Magn.* vol. 39, no. 2, pp. 981-989 (2003)
- [15] S. N. Maiti and K. Chosh, "Thermal Characteristics of Silver Powder Filled Polypropylene Composites", *Journal of Applied Polymer Science*, vol. 52, pp. 1091 - 1103, (1994).
- [16] H. Serkan Tekce, D. Kumlutas, I. H. Tavman, "Effect of Particle Shape on Thermal Conductivity of Copper Reinforced Polymer", *Composites, Journal of Reinforced Plastics and Composites*, vol. 26, no. 1, (2007)